UC Irvine

UC Irvine Previously Published Works

Title

Wound Regeneration Deficit in Rats Correlates with Low Morphogenetic Potential and Distinct Transcriptome Profile of Epidermis

Permalink

https://escholarship.org/uc/item/9dj3s4f1

Journal

Journal of Investigative Dermatology, 138(6)

ISSN

0022-202X

Authors

Guerrero-Juarez, Christian F
Astrowski, Aliaksandr A
Murad, Rabi
et al.

Publication Date

2018-06-01

DOI

10.1016/j.jid.2017.12.030

Peer reviewed

eScholarship.org Powered by the California Digital Library
University of California

Author Manuscript

Author Manuscript

Author Manuscript

Author Manuscript

HHS Public Access

Author manuscript

J Invest Dermatol. Author manuscript; available in PMC 2019 June 01.

Published in final edited form as:

J Invest Dermatol. 2018 June ; 138(6): 1409–1419. doi:10.1016/j.jid.2017.12.030.

Wound regeneration deficit in rats correlates with low morphogenetic potential and distinct transcriptome profile of epidermis

Christian F. Guerrero-Juarez[1,2,3], **Aliaksandr A. Astrowski**[4], **Rabi Murad**[1,3], **Christina T. Dang**[1,2], **Vera O. Shatrova**[4], **Aksana Astrowskaja**[4], **Chae Ho Lim**[5], **Raul Ramos**[1,2,3], **Xiaojie Wang**[1,2,3], **Yuchen Liu**[1,2], **Hye-Lim Lee**[1,2], **Kim T. Pham**[1,2], **Tsai-Ching Hsi**[1,2], **Ji Won Oh**[1,2,6,7,8], **Daniel Crocker**[9], **Ali Mortazavi**[1,3], **Mayumi Ito**[5], and **Maksim V. Plikus**[#,1,2,3]

[1]Department of Developmental and Cell Biology, University of California, Irvine, CA 92697, USA.

[2]Sue and Bill Gross Stem Cell Research Center, University of California, Irvine, CA 92697, USA.

[3]Center for Complex Biological Systems, University of California, Irvine, Irvine, CA 92697, USA.

[4]Department of Medical Biology and Genetics, Grodna State Medical University, Grodna 230009, Belarus.

[5]The Ronald O. Perelman Department of Dermatology, Department of Cell Biology, New York University School of Medicine, New York, NY 10016, USA.

[6]Department of Anatomy, School of Medicine, Kyungpook National University, Daegu, 41944, Republic of Korea.

[7]Biomedical Research Institute, Kyungpook National University Hospital, Daegu, 41944, Republic of Korea.

[8]Hair Transplantation Center, Kyungpook National University Hospital, Daegu, 41944, Republic of Korea.

[9]Department of Biology, Sonoma State University, Rohnert Park, CA 94928, USA.

Abstract

Large excisional wounds in mice prominently regenerate new hair follicles (HFs) and fat, yet humans are deficient for this regenerative behavior. Currently, wound-induced regeneration remains a clinically desirable, but only partially understood phenomenon. We show that large excisional wounds in rats, across seven strains fail to regenerate new HFs. We compared wound transcriptomes between mice and rats at the time of scab detachment, which coincides with the onset of HF regeneration in mice. In both species, wound dermis and epidermis share core dermal and epidermal transcriptional programs respectively, yet prominent inter-species differences exist. Compared to mice, rat epidermis expresses distinct transcriptional and epigenetic factors, markers

[#]Author for correspondence: Maksim V. Plikus, PhD, Department of Developmental and Cell Biology, Center for Complex Biological Systems, Sue and Bill Gross Stem Cell Research Center, University of California Irvine, Irvine, California 92697, USA, plikus@uci.edu.

Conflict of Interest

The authors declare no conflict of interest.

Author Manuscript Author Manuscript Author Manuscript Author Manuscript

of epidermal repair, hyperplasia, and inflammation, and lower levels of WNT signaling effectors and regulators. When recombined on the surface of excisional wounds with vibrissa dermal papillae, partial-thickness skin grafts containing distal pelage HF segments, but not interfollicular epidermis, readily regenerated new vibrissa-like HFs. Together, our findings establish rats as a non-regenerating rodent model for excisional wound healing and suggest that low epidermal competence and associated transcriptional profile may contribute to its regenerative deficiency. Future comparison between rat and mouse may lend further insight into the mechanism of wounding-induced regeneration and causes for its deficit.

Introduction

Full-thickness wounds in adult mammals typically repair with scarring. However, large wounds in laboratory mice *(Mus musculus)* regenerate new hair follicles (HFs) in their center. This phenomenon of wound-induced hair neogenesis (WIHN), recapitulates embryonic HF morphogenesis programs (Ito et al., 2007, Wang et al., 2015). While the cellular sources for new HFs are poorly understood (Ito et al., 2007, Snippert et al., 2010, Wang et al., 2017), the signaling and epigenetic requirements for WIHN have been partially elucidated. Critical for WIHN is canonical WNT signaling (Gay et al., 2013, Ito et al., 2007, Myung et al., 2013). Physiologically, both dermal (Gay et al., 2013) and epidermal WNT ligand sources (Myung et al., 2013) are important, and they likely act at distinct phases of WIHN. Enhanced HF neogenesis in wounds of mice from the genus *Acomys* is also positively correlated with high WNT activity (Seifert et al., 2012). Other signals also play a role in WIHN. Dermal WNT signaling is driven by Fgf9, initially secreted by γδ T-cells (Gay et al., 2013). Also important for WIHN is Tlr3 signaling and its downstream effectors Il6 and Stat3 (Nelson et al., 2015). Tlr3 is activated by the double-stranded RNA released from damaged keratinocytes at the onset of wound healing. Promoting WIHN downstream of Il6/Stat3 signaling is TAp63, a p63 isoform (Nelson et al., 2016). WIHN efficiency is also negatively regulated by prostaglandin Pdg2 signaling (Nelson et al., 2013), Cxxc5 transcriptional regulator (Lee et al., 2017) and Msi2 RNA-binding protein (Ma et al., 2017), and modulated by the macrophage-derived Tnfα signaling via TNF/p-AKT/p-β-catenin pathway (Wang et al., 2017).

Apart from mice, definitive WIHN has been shown only in rabbits (Billingham and Russell, 1956, Breedis, 1954, Stenbäck et al., 1967). Although suggested to take place in sheep, the reported evidence for WIHN was inconclusive (Brook et al., 1960). In humans, Kligman and Strauss (1956) reported regeneration of sparse vellus HFs in the facial skin following partial freezing and dermabrasion. However, robust regeneration of new HFs in human wounds is generally not observed (Gay et al., 2013).

In this study, we asked if WIHN occurs in laboratory rats (*Rattus norvegicus)* and how this process compares to that in mice. This inquiry was stimulated by the contradicting reports in the classic literature on the outcomes of rat skin repair following cryo-injury. While Taylor (1949) and Mikhail (1963) suggested that cryo-damaged skin in rats repairs with HF neogenesis, Stenbäck et al. (1967) failed to replicate these findings. We now show that rats distinctly fail to regenerate new HFs in large full-thickness excisional wounds. We further

Author Manuscript Author Manuscript Author Manuscript Author Manuscript

explore non-regenerative wound healing in rats with the means of inter-species comparative transcriptomic analyses and tissues recombination experiments.

Results

Rats fail to regenerate new hair follicles and fat in large skin wounds.

Large excisional wounds in adult mice regenerate new HFs soon after re-epithelialization, around post-wounding day (PWD) 15 (Gay et al., 2013, Ito et al., 2007), and new adipocytes surrounding neogenic HFs from PWD21 onward (Plikus et al., 2017) (Figure 1a). We tested if large excisional wounds in adult rats similarly regenerate new HFs and fat. In rats (outbred Sprague-Dawley strain), wounds were made larger (circular d=2.0 cm) than in mice (squared s=1.5 cm) and complete re-epithelialization, as measured by the timing of scab detachment, took comparatively longer, 30.0+/−1.0 days. However, no neogenic HFs were observed in all animals when examined at PWD40 (n=5) (Figure 1b and 1c). Because WIHN efficiency in mice can vary across strains (Nelson et al., 2013), we next compared wound repair outcomes across six other strains of rats. In addition to Sprague-Dawley, we examined three outbred strains: CD IGS (n=5), Long-Evans (n=5), Wistar (n=5) and three inbred rats: F344 FISCH (n=5), Brown Norway (n=3), Buffalo (n=5). The timing of wound re-epithelialization varied significantly across the strains (P=0.0011) with a range of 25–33 days (Figure 1b; Table S1). Compared to mice (number of regenerated hair follicles=15±5.85), all rats studied consistently failed to undergo WIHN (P=0.0127) (Figure 1c). Absence of neogenic HFs in PWD40 wounds was further validated in Sprague-Dawley rats (n=4) by Krt17 (Figure 1d *vs.* 1h) and alkaline phosphatase whole-mount staining (Figure 1e *vs.* 1i), and in several other rat strains by histology (Figure S1). Commonly, wound epidermis formed small peg-like projections (Figure S1b, S1c), however these displayed clear epidermal, rather than HF, organization.

Next, we considered that relatively large wounds, with their extended re-epithelialization dynamics, could be incompatible with WIHN. We addressed this possibility by studying repair outcomes of smaller squared s=1.5 cm and s=1.0 cm wounds in Sprague-Dawley (n=5 and n=4 respectively) and CD IGS rats (n=5 and n=5 respectively). Surprisingly, we observed generally slower wound re-epithelialization dynamics as compared to these in mice, and all wounds studied failed to undergo WIHN by PWD40 (Tables S2, S3). Lack of neogenic HFs was further confirmed on Krt17 and alkaline phosphatase whole-mount staining (Figure S2). Consistent with a recent report in mice (Plikus et al., 2017), hairless wounds in rats failed to regenerate new adipocytes (Figure 1g). These observations suggest that rat is a suitable rodent model for studying non-regenerative healing of large excisional skin wounds.

Wound transcriptome profiling reveals rat and mouse specific gene expression patterns.

To identify molecular signatures that underlie regenerative behavior differences between rats and mice, we studied transcriptomes of wound epidermis and dermis collected at the time of complete re-epithelialization. Inter-species transcriptome analysis was performed using mouse and rat one-to-one orthologs and principal component analysis (PCA) revealed significant separation between all tissue types, yet close clustering of biological replicates

Author Manuscript Author Manuscript Author Manuscript Author Manuscript

(Figure 2a). To resolve the transcriptome of mouse *vs.* rat wound tissues, we utilized the Bioconductor package edgeR (Li and Dewey, 2011). We identified 3,850 differentially expressed gene orthologs (DEGOs) (5% FDR level, minimum 4X-fold change) that grouped into eight distinct clusters (Figure 2b). Clusters 1 and 2 include DEGOs upregulated in both species in wound epidermis and dermis, respectively (*aka* shared epidermal and dermal genes). Cluster 3 identifies mouse-specific and cluster 4 – rat-specific epidermal DEGOs, while clusters 5 and 6 identify mouse- and rat-specific dermal DEGOs, respectively. Finally, cluster 7 contains mouse-specific DEGOs upregulated both in epidermis and dermis, while cluster 8 contains rat-specific DEGOs (Table S9).

Next, we examined shared epidermal and dermal genes and show that these include multiple established markers of epidermal and dermal lineages, respectively. On pathway analysis, epidermal cluster 1 is enriched for terms such as keratinocyte proliferation, keratinocyte differentiation, skin barrier, phospholipid metabolism and wound healing (Figure 2c; Table S10) while dermal cluster 2 is enriched for terms such as extracellular matrix, cell-matrix adhesion, leukocyte migration, wound healing, WNT and BMP signaling (Figure 2c; Table S10). Rat and mouse wound epidermis share core transcriptional regulators of the epidermal lineage (Cebpb, Gata3, Grhl2, Grhl3, Irf6, Klf4/5, Ovol1, Vdr, Zfp750), key early epidermal differentiation markers (*Cnfn, Evpl, Krt1, Krt14, Krt15, Krt16, Tgm1, Tgm5*) and epidermal adhesion molecules (Cdh1, Col17a1, Dsc1, Dsc3, Dsp, Epcam, Itga6, Lamb3, Ocln, Pkp1, Pkp3) (Figure S3a). Rat and mouse wound dermis share multiple mesenchymal transcriptional regulators (*En1, Meox1, Meox2, Snai1, Tbx15*) and extracellular matrix proteins (*Col1a1, Col3a1, Col5a1, Col6a1*) (Figure S3b). At the same time, notable species-specific differences are present. Rat wound epidermal DEGOs include *Notch1, Krt17* and transcriptional regulators *Hopx, Hr, Id4, Sox9* (Figure 2d). Hopx (Takeda et al., 2013) and Sox9 (Vidal et al., 2005) mark HF stem cells in unwounded mouse skin and given the non-regenerative characteristics of rat wounds, their elevated expression in rat epidermis, including on immunostaining (Figure S3e), appears paradoxical. However, Hopx (Mariotto et al., 2016) and Sox9 (Shi et al., 2013) can also regulate epidermal lineage program in humans, and similar to Sox9 (Shi et al., 2013), elevated Krt17 (Depianto et al., 2010) and Notch1 expression (Li et al., 2016) correlate with epidermal repair, hyperplasia and inflammation. Mouse epidermal DEGOs include *Cebpa, Dlx3, Dlx5, Sox7* and *Tcf23* (Figure 2e). Of these, Cebpa (Lopez et al., 2009) and Dlx3 (Hwang et al., 2011) reduce epidermal hyperplasia and inflammation, and promote differentiation. Consistently, on pathway analysis, rat wound epidermis is enriched for epithelial migration and proliferation terms, while mouse wound epidermis shows enrichment for lipid biosynthesis terms, including cholesterol synthesis typically associated with terminal differentiation (Figure 2c; Table S10). Therefore, we posit that, compared to mouse, rat wound epidermis is less mature at the time of scab detachment.

Regarding the species-specific differences in wound dermis, rats express higher levels of transcriptional regulator *Runx2*, implicated in keloid scarring (Hsu et al., 2017), and extracellular matrix proteins *Col5a3, Des* and *Tnn* (Figure 2f), while mice express higher levels of transcriptional regulators *Dnmt3a, Hdac7, Sox18,* contractile proteins *Acta2, Afap1* and collagens *Col26a1, Col27a1* (Figure 2g).

Author Manuscript Author Manuscript Author Manuscript Author Manuscript

We also compared rat and mouse wounds in terms of the signaling activities implicated in HF development and regeneration. Prominently, we observe species-specific differences in canonical WNT signaling. While in both species, canonical WNT ligands *Wnt3, Wnt4* and *Wnt7b* are expressed in wound epidermis (Figures S3a) and soluble WNT inhibitors *Dkk3, Sfrp2* and *Sfrp4* in wound dermis (Figures S3b), only mouse wounds (both epidermis and dermis) show high expression of *Axin2,* a direct WNT signaling target (Figure S3d). Furthermore, compared to rats, mouse wound epidermis shows higher expression of the negative WNT signaling regulators, *Ctnnbip1* and *Kremen2* (Figure 2e). In terms of BMP signaling, both species express *Bmp7* in wound epidermis, while wound dermis expresses BMP antagonists *Chrdl2, Grem1* and *Grem2* (Figure S3a, S3b). Additionally, in rats, epidermis expresses the BMP antagonist *Sostdc1*, while mouse dermis expresses *Bmp4*. No prominent inter-species differences are seen for the FGF and SHH pathways. Among the pathways not implicated in HF development, mouse wounds show expression patterns consistent with higher IGF/insulin and TGFβ signaling, and distinct repertoire of immune cytokines.

Lastly, we evaluated epigenetic factors. Rat wounds overexpress chromatin modifiers regulating epidermal differentiation *Satb1* (Fessing et al., 2011), *Smarca4* (Mardaryev et al., 2014), and *Cbx2, Kdm8, Rbbp4, Setdb1*. Mouse wounds overexpress Dnmt3a, Hdac4, Ing5, Kdm2a, Mysm1, Setd1b, Smyd4, Whsc1l1 (Table S9). Select epigenetic factors were further validated by qRT-PCR (Rat/Mouse F.C., $P<0.05$) (Figure 2i) and immunostaining (Figure 2j–2k; Text S1). These analyses suggest that despite sharing core transcriptional programs, wound epidermis in rats appears to be less mature, less WNT responsive, and potentially, less competent as compared to mice.

Rat interfollicular epidermis fails to regenerate hair follicles in tissue recombination experiments.

To further investigate if HF regeneration deficit in rat wounds relates to low epidermal competence, we designed autologous tissue recombination assays in which inter-follicular epidermis (IFE) is co-transplanted with vibrissa dermal papillae (DPs) onto the surface of circular, $d = 2.0$ cm wound (Figure 3a). Briefly, in this assay a full-thickness wound is created on the dorsal skin inside of an isolating chamber. DPs are microdissected from vibrissae HFs and grafted onto the wound surface. Lastly, an intact sheet of IFE is isolated from the animal's flank using vacuum-suction and transferred in an unfolded state on top of the grafted DPs using adhesive semi-dissolvable carrier (Figure S4, S5). This model enables studying regenerative responses of epidermis to hair-inducing DPs within wound settings.

We evaluated interaction outcomes between IFE and DPs on post-grafting days 3, 5, 7, 10, 14 and 20 (n=5 per time point; ≥ 10 DP per experiment). Following grafting, IFE underwent transient hyperproliferation (Figure S6), increased in thickness (Figure S7) and reformed the basal membrane (Figure S8). By day 7, IFE formed prominent pocket-like invaginations surrounding DPs (Figure 3d). However, no neogenic HFs formed even by day 20 (Figure 3e–3h). We then considered that hair-inducing properties of DPs may change with respect to the hair growth cycle, as previously shown in the vibrissa amputation model (Iida et al., 2007). We tested DPs derived from eight different time points, comprehensively covering the entire

Author Manuscript Author Manuscript Author Manuscript Author Manuscript

vibrissa hair cycle. We synchronized donor vibrissae by plucking (Figure S9) and grafted micro-dissected DPs as follow: post-plucking week 1 – latent period; weeks 2, 3 – early anagen; weeks 4, 5 – mid-anagen; week 6 – late anagen; week 7 – catagen/telogen and week 8 – second early anagen. We analyzed the resulting morphogenetic interactions on day 10 (n=5 per time point; ≥ 10 DP per experiment) and day 20 (n=5 per time point; ≥ 10 DP per experiment). First, we found that transplanted DPs generally preserved their relative sizes, such that initially larger anagen DPs maintained greater volume as compared to initially smaller telogen DPs both on day 10 and day 20 (Tables S6, S7). Secondly, the extent of DP-IFE interactions changed as a function of hair cycle with a statistically larger portion of anagen DPs contacting IFE as compared to telogen DPs, both at day 10 (P=0.002) and day 20 (P=0.0039) (Table S8). Lastly, for all eight hair cycle time points tested, no morphologically recognizable neogenic HFs were induced at the sites of DP-IFE interactions.

Next, we asked if DPs alter the differentiation signature of the grafted IFE. On immunostaining of rat vibrissa HFs, Krt14 is expressed in IFE, infundibulum, and suprabasal layers of the outer root sheath (ORS) (Figure 4a). It is largely absent from hair matrix, precortex, inner root sheath (IRS), and hair fiber (Figure 4b). Krt10, the hallmark suprabasal IFE marker, is not expressed in normal vibrissa HFs with the exception of the distal infundibulum (Figure 4e, 4f). In contrast, DP-IFE structures in grafts distinctly expressed both Krt14 (Figure 4c, 4d) and Krt10 (Figure 4g, 4h). Hair cytokeratin markers AE13 and AE14, normally expressed in the differentiating hair shaft (Figure 4i, 4j), were distinctly absent from DP-IFE structures (Figure 4k, 4l). In addition, hyperplastic epidermis within DP-IFE structures showed a high number of PCNA-positive cells (Figure S10d *vs.* S10c), yet no nuclear β-catenin expression (Figure S10h).

Despite failing to regenerate new HFs, in rare instances DP-IFE interactions occurred some distance away from the surface and produced cup-like structures morphologically reminiscent of the hair peg stage of normal HF morphogenesis (Figure 3k). We considered that failure to regenerate HFs can relate to the lack of proper spatial conditions for morphogenetic interactions, such as the conditions enabling epithelial downgrowth. To test for this possibility, we modified our model to include a devitalized dermal scaffold placed in between DPs and IFE (Figure 5a). In this model, grafted IFE invades vacant canals of the scaffold on days 3–5 and then retracts by day 20 (Figure S11). Epidermal strands can interact with the DPs within the scaffold (Figure 5b–5d). However, the resulting DP-IFE structures do not become HFs, but instead form keratin pearls (n=3) (Figure 5d, 5e). Taken together, we show that rat epidermis fails to regenerate new HFs or activate hair-specific differentiation program in response to DPs in this wound reconstitution assay.

Interfollicular and wound epidermis have distinct, but largely overlapping transcriptomes.

Considering that no HFs regenerate in rats spontaneously from wound epidermis or from wound-grafted IFE under the influence of DPs, we thought to compare their transcriptomes (Figure S12; Table S11). Expression differences are observed among transcriptional factors, with IFE upregulating *Foxo1/3, Klf2, Nfatc2, Rora, Rxra* and *Stat5a/5b* and wound epidermis upregulating *Cebpb, Fhl2, Foxp1, Nfkb1, Pitx1, Runx1, Sox9* and *Stat1*. Apart

Author Manuscript Author Manuscript Author Manuscript Author Manuscript

from *Wnt7b* in IFE, no substantial expression differences are observed for other canonical WNT ligands and antagonists; yet wound epidermis distinctly upregulates several non-canonical WNT pathway members, *Wnt4, Wnt11* and *Fzd6*. The latter also upregulates BMP antagonists *Fstl1* and *Sostdc1* and VEGF ligands *Vegfa, Vegfb*. Expression differences are also observed for some members of TGFβ pathway and immune cytokines, without clear epidermal type preferences (Figure S12). Together, albeit different in some respects, gene expression across the key pathways implicated in HF development is largely similar between the IFE and wound epidermis and the observed differences, including *Sox9*, *Wnt4* and *Wnt11* differences, do not positively correlate with the regenerative potential of epidermis.

DPs induce vibrissa-like HFs from split-thickness dorsal skin grafts.

Lastly, we further confirmed that lack of HF regeneration in our wound model was not because of the lack of DP inductivity. We substituted adult IFE for split-thickness dorsal skin grafts (Figure 6a). Giant, vibrissa-like HFs consistently formed when either anagen (n=6; ≥ 10 DPs per experiment) or telogen DPs (n=5; ≥ 10 DPs per experiment) came in contact with hair-fated epithelium of distal pelage HF segments of the grafts. Commonly, regenerated HFs had a bifurcated appearance, likely due to DPs interacting with more than one HF segment (Figures 6b, S13). Anagen DPs were nearly twice as efficient at inducing HF regeneration in comparison to telogen DPs (97.7% *vs*. 65.4% HF induction efficiency). Pelage HF segments not in contact with vibrissa DPs failed to regenerate HFs, and small epidermal cysts formed instead (Figure 6b, arrowheads). To further test the robustness of DP inductive properties, we performed grafting using DPs isolated from donor vibrissae, previously focally irradiated with 24Gy of X-ray, which resulted in permanent HF degeneration. DPs, however, survived the irradiation and could be located at the base of the remaining collagen capsule (Figure 6c *vs.* 6d). In combination with split-thickness skin grafts, irradiated DPs induced vibrissa-like HFs (n=8; 6 DPs per experiment) with the success rate of 61.9% (Figure 6e). Together, this data shows that lack of HF regeneration in the recombination experiments relates to low epidermal competence rather than poor vibrissa DP inductivity.

Discussion

In mice, neogenesis of HFs (Ito et al., 2007) and adipocytes (Plikus et al., 2017) in large excisional wounds shifts the repair process away from scarring and toward embryonic-like regeneration. Unlike mice, however, humans rarely show signs of neogenesis (Kligman and Strauss, 1956) and commonly heal with scarring (Gay et al., 2013, van den Broek et al., 2014). Therefore, regeneration of HFs and fat remains a desirable, yet clinically unmet outcome of wound repair and understanding the basis for WIHN and its failure constitutes an important research question.

Non-regenerative healing in rats establishes a new paradigm for future WIHN studies through cross-species comparison with mice. This approach is facilitated by close evolutionary distance (Kimura et al., 2015) and similar skin anatomy between rats and mice. Our analyses already show that transcriptomic profiles substantially differ between the two species at the time of complete wound re-epithelialization. Rat wound epidermis upregulates

Author Manuscript Author Manuscript Author Manuscript Author Manuscript

distinct transcriptional and epigenetic factors from that of mice. Rats also overexpress *Notch1* and *Krt17*. Considering the role of Sox9 (Shi et al., 2013), Krt17 (Depianto et al., 2010) and Notch1 (Li et al., 2016) in epidermal hyperplasia and inflammation, and that of Cebpa (Lopez et al., 2009) and Dlx3 (Hwang et al., 2011) in their reduction, we conclude that wound epidermis in rats is immature and, likely, not competent for HF neogenesis. Our tissue reconstitution studies further support this notion. Future works will be required to explore the impact of inter-species differences in wound dermis. To this end, our transcriptomic data already points toward significant inter-species differences in the dermal wound compartment.

We place our findings in the context of the classic works on wound healing and tissue recombination. Our findings generally agree with these by Stenbäck et al. (1967) that full-thickness wounds in rats cannot regenerate new HFs, however, new inquiry into the cryo-injury wounding model is warranted. In terms of the reconstitution assays, new HFs were shown to form from non-hair fated adult epidermis (Jahoda, 1992, Jahoda et al., 1993, McElwee et al., 2003, Reynolds and Jahoda, 1992). Nonetheless, when tested in the context of well-controlled experimental conditions, HF-forming abilities of non-hair fated epidermis are on an order of magnitude lower than those of hair-fated epithelia (Ehama et al., 2007, Ferraris et al., 1997, Yang and Cotsarelis, 2010). Our data reveals a general failure of adult rat IFE to reconstitute HFs in the presence of DPs, while vibrissa-like HFs are readily induced by the DPs from hair-fated epithelium. Reflecting on these differences with the classic literature, we note that our vacuum-assisted IFE isolation technique minimized contamination for HF epithelium, while prior experimental models contained endogenous HFs (ear pinna slit-wound model), or included hair-fated epithelial cells (enzymatically-digested newborn skin epithelium).

In conclusion, our studies reveal an inability of excisional wounds in rats to undergo WIHN and implicate low epidermal competence and its associated gene expression signature as the possible contributing factors. We also establish non-regenerating rat *vs.* regenerating mouse wound comparison as the new experimental paradigm for studying the basis for HF neogenesis.

Materials and Methods

Wounding procedures.

All animal procedures were approved by IACUC. Wounding was performed as previously described (Ito et al., 2007). One wound was created per animal, in 4-to-8 week-old mice and 5-to-7 week-old rats. Wounds healed by secondary intention. See Supplement for further experimental details.

Autologous transplantation.

Full-thickness circular wounds were introduced in the rat dorsum and isolated with a plastic chamber. Autologous IFE was obtained using vacuum suction (Figure S4). Epidermis was transferred using an adhesive semi-dissolvable cellophane carrier (Figure S5). Microdissected DPs were transferred onto the surface of the wound and IFE was placed on

Author Manuscript Author Manuscript Author Manuscript Author Manuscript

top, basal layer side down. In subsequent versions of transplantation assays, a devitalized dermal scaffold was placed between DPs and IFE. In another modification, split-thickness dorsal skin was placed on top of the transplanted DPs. Wounded animals were monitored every 72 hours. See Supplement for further experimental details.

Supplementary Material

Refer to Web version on PubMed Central for supplementary material.

Acknowledgements

MVP is supported by Pew Charitable Trust grant and NIH grants R01-AR067273 and R01-AR069653, CFGJ is supported by NSF-GRFP (DGE-1321846) and MBRS-IMSD training grant (GM055246), JWO is supported by the National Research Foundation of Korea (NRF) grant funded by the Korea government (MSIP) (2016R1C1B1015211), HLL is supported by NIH NCI T32 training grant (T32-CA009054).

References

Billingham RE, Russell PS. Incomplete wound contracture and the phenomenon of hair neogenesis in rabbits' skin. Nature 1956;177(4513):791–2.

Breedis C Regeneration of hair follicles and sebaceous glands from the epithelium of scars in the rabbit. Cancer research 1954;14(8):575–9.13199800

Brook AH, Short BF, Lyne AG. Formation of new wool follicles in the adult sheep. Nature 1960;185:51.

Depianto D, Kerns ML, Dlugosz AA, Coulombe PA. Keratin 17 promotes epithelial proliferation and tumor growth by polarizing the immune response in skin. Nat Genet 2010;42(10):910–4.20871598

Ehama R, Ishimatsu-Tsuji Y, Iriyama S, Ideta R, Soma T, Yano K, Hair follicle regeneration using grafted rodent and human cells. The Journal of investigative dermatology 2007;127(9):2106–15.17429436

Ferraris C, Bernard BA, Dhouailly D. Adult epidermal keratinocytes are endowed with pilosebaceous forming abilities. Int J Dev Biol 1997;41(3):491–8.9240566

Fessing MY, Mardaryev AN, Gdula MR, Sharov AA, Sharova TY, Rapisarda V, p63 regulates Satb1 to control tissue-specific chromatin remodeling during development of the epidermis. J Cell Biol 2011;194(6):825–39.21930775

Gay D, Kwon O, Zhang Z, Spata M, Plikus MV, Holler PD, Fgf9 from dermal gammadelta T cells induces hair follicle neogenesis after wounding. Nature medicine 2013;19(7):916–23.

Hsu CK, Lin HH, H ICH, Ogawa R, Wang YK, Ho YT, Caveolin-1 controls hyperresponsiveness to mechanical stimuli and fibrogenesis-associated RUNX2 activation in keloid fibroblasts. The Journal of investigative dermatology 2017.

Hwang J, Kita R, Kwon HS, Choi EH, Lee SH, Udey MC, Epidermal ablation of Dlx3 is linked to IL-17-associated skin inflammation. Proc Natl Acad Sci U S A 2011;108(28):11566–71.21709238

Iida M, Ihara S, Matsuzaki T. Follicular epithelia and dermal papillae of mouse vibrissal follicles qualitatively change their hair-forming ability during anagen. Differentiation; research in biological diversity 2007;75(5):371–81.17286596

Ito M, Yang Z, Andl T, Cui C, Kim N, Millar SE, Wnt-dependent de novo hair follicle regeneration in adult mouse skin after wounding. Nature 2007;447(7142):316–20.17507982

Jahoda CA. Induction of follicle formation and hair growth by vibrissa dermal papillae implanted into rat ear wounds: vibrissa-type fibres are specified. Development 1992;115(4):1103–9.1451660

Jahoda CA, Reynolds AJ, Oliver RF. Induction of hair growth in ear wounds by cultured dermal papilla cells. The Journal of investigative dermatology 1993;101(4):584–90.8409527

Kimura Y, Hawkins MT, McDonough MM, Jacobs LL, Flynn LJ. Corrected placement of Mus-Rattus fossil calibration forces precision in the molecular tree of rodents. Sci Rep 2015;5:14444.26411391

Author Manuscript Author Manuscript Author Manuscript Author Manuscript

Kligman AM, Strauss JS. The formation of vellus hair follicles from human adult epidermis. The Journal of investigative dermatology 1956;27(1):19–23.13357817

Lee SH, Seo SH, Lee DH, Pi LQ, Lee WS, Choi KY. Targeting of CXXC5 by a Competing Peptide Stimulates Hair Regrowth and Wound-Induced Hair Neogenesis. The Journal of investigative dermatology 2017;137(11):2260–9.28595998

Li B, Dewey CN. RSEM: accurate transcript quantification from RNA-Seq data with or without a reference genome. BMC bioinformatics 2011;12:323.21816040

Li Z, Hodgkinson T, Gothard EJ, Boroumand S, Lamb R, Cummins I, Epidermal Notch1 recruits RORgamma(+) group 3 innate lymphoid cells to orchestrate normal skin repair. Nature communications 2016;7:11394.

Lopez RG, Garcia-Silva S, Moore SJ, Bereshchenko O, Martinez-Cruz AB, Ermakova O, C/EBPalpha and beta couple interfollicular keratinocyte proliferation arrest to commitment and terminal differentiation. Nat Cell Biol 2009;11(10):1181–90.19749746

Ma X, Tian Y, Song Y, Shi J, Xu J, Xiong K, Msi2 Maintains Quiescent State of Hair Follicle Stem Cells by Directly Repressing the Hh Signaling Pathway. The Journal of investigative dermatology 2017;137(5):1015–24.28143780

Mardaryev AN, Gdula MR, Yarker JL, Emelianov VU, Poterlowicz K, Sharov AA, p63 and Brg1 control developmentally regulated higher-order chromatin remodelling at the epidermal differentiation complex locus in epidermal progenitor cells. Development 2014;141(1):101–11.24346698

Mariotto A, Pavlova O, Park HS, Huber M, Hohl D. HOPX: The Unusual Homeodomain-Containing Protein. The Journal of investigative dermatology 2016;136(5):905–11.27017330

McElwee KJ, Kissling S, Wenzel E, Huth A, Hoffmann R. Cultured peribulbar dermal sheath cells can induce hair follicle development and contribute to the dermal sheath and dermal papilla. The Journal of investigative dermatology 2003;121(6):1267–75.14675169

Mikhail GR. Hair Neogenesis in Rat Skin. Archives of dermatology 1963;88:713–28.14071440

Myung PS, Takeo M, Ito M, Atit RP. Epithelial Wnt ligand secretion is required for adult hair follicle growth and regeneration. The Journal of investigative dermatology 2013;133(1):31–41.22810306

Nelson AM, Katseff AS, Ratliff TS, Garza LA. Interleukin 6 and STAT3 regulate p63 isoform expression in keratinocytes during regeneration. Experimental dermatology 2016;25(2):155–7.26566817

Nelson AM, Loy DE, Lawson JA, Katseff AS, Fitzgerald GA, Garza LA. Prostaglandin D2 inhibits wound-induced hair follicle neogenesis through the receptor, Gpr44. The Journal of investigative dermatology 2013;133(4):881–9.23190891

Nelson AM, Reddy SK, Ratliff TS, Hossain MZ, Katseff AS, Zhu AS, dsRNA Released by Tissue Damage Activates TLR3 to Drive Skin Regeneration. Cell stem cell 2015;17(2):139–51.26253200

Plikus MV, Guerrero-Juarez CF, Ito M, Li YR, Dedhia PH, Zheng Y, Regeneration of fat cells from myofibroblasts during wound healing. Science 2017;355(6326):748–52.28059714

Reynolds AJ, Jahoda CA. Cultured dermal papilla cells induce follicle formation and hair growth by transdifferentiation of an adult epidermis. Development 1992;115(2):587–93.1425341

Seifert AW, Kiama SG, Seifert MG, Goheen JR, Palmer TM, Maden M. Skin shedding and tissue regeneration in African spiny mice (Acomys). Nature 2012;489(7417):561–5.23018966

Shi G, Sohn KC, Li Z, Choi DK, Park YM, Kim JH, Expression and functional role of Sox9 in human epidermal keratinocytes. PLoS One 2013;8(1):e54355.23349860

Snippert HJ, Haegebarth A, Kasper M, Jaks V, van Es JH, Barker N, Lgr6 marks stem cells in the hair follicle that generate all cell lineages of the skin. Science 2010;327(5971):1385–9.20223988

Stenbäck F, Niinimäki T, Dammert K. HAIR NEOGENESIS IN RAT AND RABBIT SKIN. Acta Pathologica Microbiologica Scandinavica 1967;69(3):480–.

Takeda N, Jain R, Leboeuf MR, Padmanabhan A, Wang Q, Li L, Hopx expression defines a subset of multipotent hair follicle stem cells and a progenitor population primed to give rise to K6+ niche cells. Development 2013;140(8):1655–64.23487314

Taylor AC. Survival of rat skin and changes in hair pigmentation following freezing. J Exp Zool 1949;110(1):77–111.18113442

Author Manuscript Author Manuscript Author Manuscript Author Manuscript

van den Broek LJ, Limandjaja GC, Niessen FB, Gibbs S. Human hypertrophic and keloid scar models: principles, limitations and future challenges from a tissue engineering perspective. Experimental dermatology 2014;23(6):382–6.24750541

Vidal VP, Chaboissier MC, Lutzkendorf S, Cotsarelis G, Mill P, Hui CC, Sox9 is essential for outer root sheath differentiation and the formation of the hair stem cell compartment. Curr Biol 2005;15(15):1340–51.16085486

Wang X, Chen H, Tian R, Zhang Y, Drutskaya MS, Wang C, Macrophages induce AKT/beta-catenin-dependent Lgr5+ stem cell activation and hair follicle regeneration through TNF. Nature communications 2017;8:14091.

Wang X, Hsi TC, Guerrero-Juarez CF, Pham K, Cho K, McCusker CD, Principles and mechanisms of regeneration in the mouse model for wound-induced hair follicle neogenesis. Regeneration (Oxf) 2015;2(4):169–81.26504521

Yang CC, Cotsarelis G. Review of hair follicle dermal cells. J Dermatol Sci 2010;57(1):2–11.20022473

Author Manuscript Author Manuscript Author Manuscript Author Manuscript

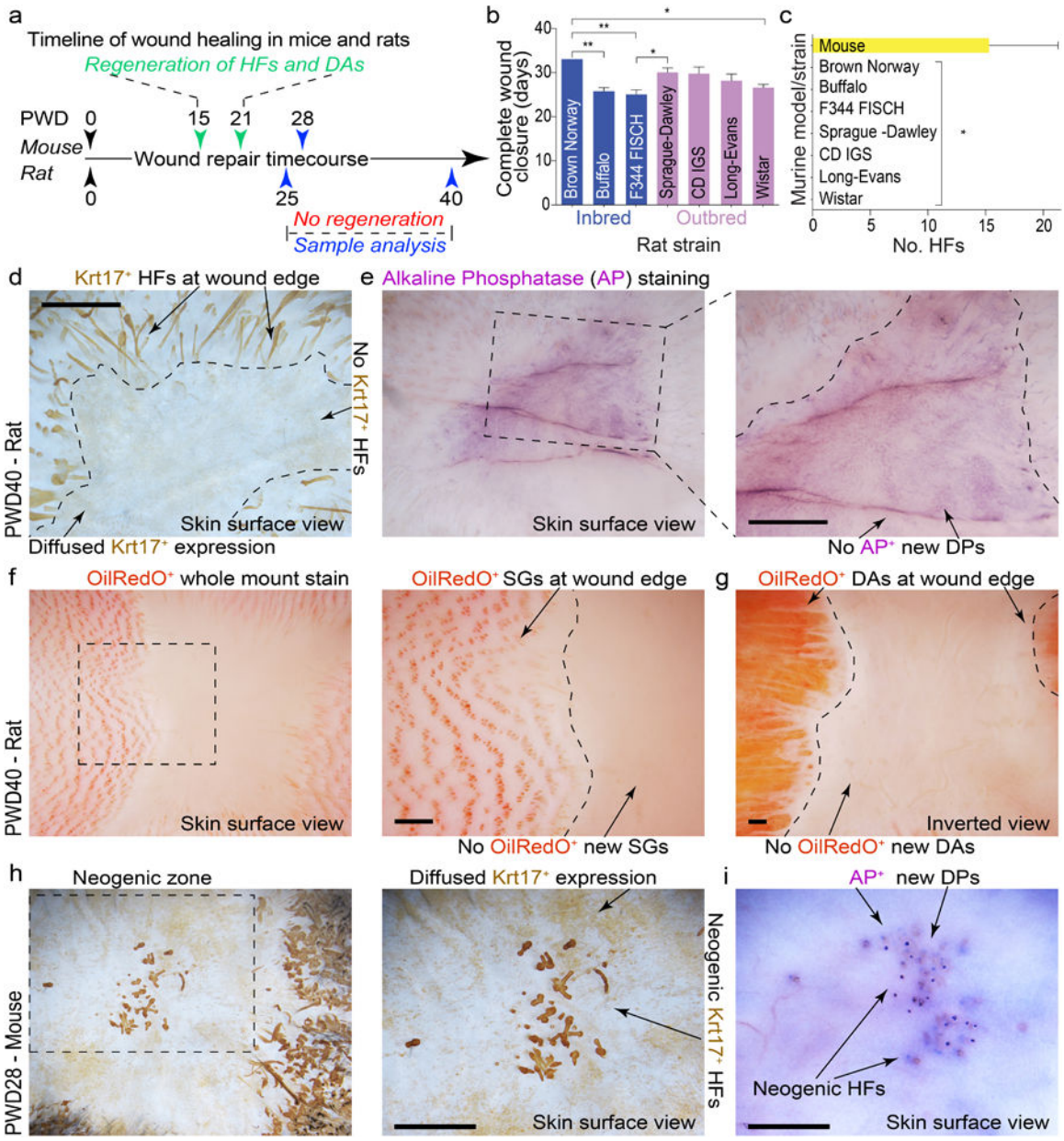

Figure 1: Adult rats fail to regenerate new hair follicles and new adipocytes after excisional wounding.

(a) Timeline of full-thickness excisional wound healing in mice and rats. Mouse wounds heal and regenerate new HFs and dermal adipocytes (DA), while rat wounds fail to regenerate. **(b)** Despite their inability to regenerate, circular (*d*=2.0 cm) wounds in rats (see Table S1 for biological replicate information) undergo complete re-epithelialization, ranging between 25–33 days depending on the strain (see Table S1 for details). **(c)** Circular *d*=2.0 cm wounds in all strains of rats (n=5 per strain) failed to regenerate new HFs and new DA. Wounds in three out of five mixed background mice regenerated new HFs. Of these three mice, average number of regenerated HFs was 15 (see Tables S4 and S4). **(d, e)** Wholemount Krt17 and alkaline phosphatase (AP) staining revealed lack of new HFs in

Author Manuscript Author Manuscript Author Manuscript Author Manuscript

circular excisional wounds in rats at PWD40. Representative wounds are shown. **(f, g)** Wholemount OilRedO staining confirms the absence of new HFs (based on the lack of $OilRedO^+$ sebaceous glands (SGs)) and new DA in circular excisional wounds in rats at PWD40. Representative wound is shown. **(h, i)** Wholemount Krt17 and AP staining reveal new HFs in excisional wounds in mice at PWD28. Representative wounds that underwent HF regeneration are shown. Values in the graphs on 1b and 1c are means ± S.E.M. One-way ANOVA in 1b, $P<0.05$; Post-hoc Tukey's multiple comparison test in 1b, $*P<0.05$, $**P<0.01$; two-tailed unpaired *t*-test in 1c, $*P=0.0127$. Size bars: d-j – 100 μm.

Author Manuscript
Author Manuscript
Author Manuscript
Author Manuscript

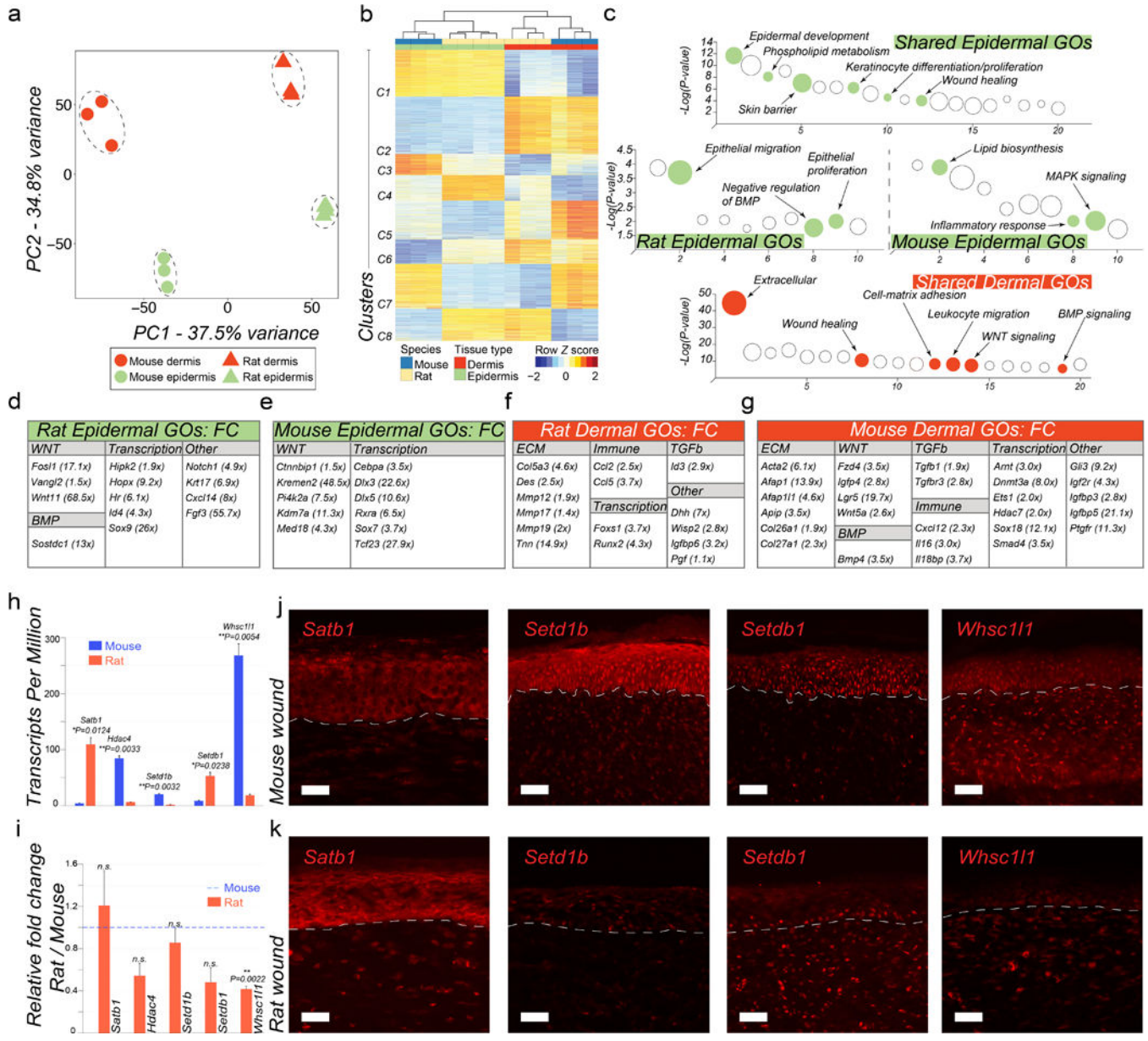

Figure 2: Transcriptome analyses of wound epidermis and dermis between mice and rats.

(a) Principal Component Analysis (PCA) reveals distinct separation between tissue types (wound epidermis and dermis) and between species (mouse *vs.* rat wound tissues). **(b)** Heat map representing 3,850 differentially expressed one-to-one gene orthologs between mouse and rat wound tissues grouped into eight different clusters. **(c)** Pathway analysis on gene clusters #1 (shared epidermal genes), #2 (shared dermal genes), #3 (mouse-specific epidermal genes) and #4 (rat-specific epidermal genes). Select pathways are marked (see Table S10) **(d, e)** Display of rat and mouse gene orthologs upregulated in wound epidermis. **(f, g)** Display of rat and mouse gene orthologs upregulated in wound dermis. **(h)** Rat and mouse TPM values for select epigenetic factors from RNA-seq (see Table S9). **(i)** qRT-PCR validation of select differentially expressed epigenetic factors between rat and mouse wound epidermis, including *Satb1, Hdac4, Setd1b, Setdb1* and *Whsc1l1*. **(j, k)** Immunostaining of

Author Manuscript Author Manuscript Author Manuscript Author Manuscript

mouse **(j)** and rat wounds **(k)** at the time of scab detachment for select epigenetic factors: Satb1, Setd1b, Setdb1 and Whsc1l1. See Text S1 for detailed description of the observed expression pattern in wounds. Differential gene ortholog expression identification was performed at 5% FDR level and minimum 4X-fold change. Values in the graphs on 2h and 2i are means ± S.E.M. Two-tailed paired *t*-test in 2h, **P*=0.0124 for *Satb1*, ***P*=0.0033 for *Hdac4*, ***P*=0.0032 for *Setd1b*, **P*=0.0238 for *Setdb1*, ***P*=0.0054 for *Whsc1l1*; and in 2i, ***P*=0.0022. Size bars: j, k – 25 μm.

Author Manuscript Author Manuscript Author Manuscript Author Manuscript

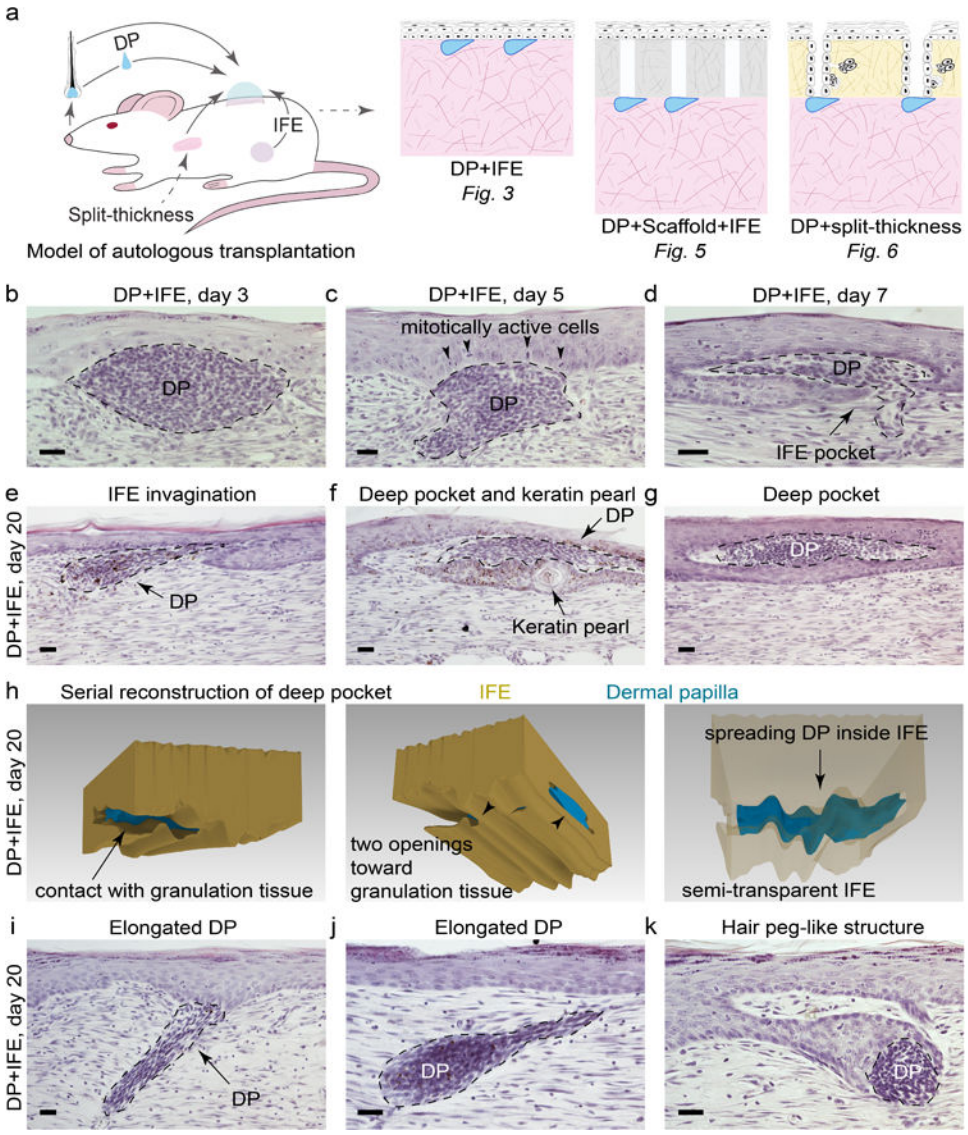

Figure 3: Characterization of dermal papilla-epidermal interactions in the wound of rats.

(a) Experimental design and tissue grafting scenarios used in this study. **(b-d)** Upon co-transplantation with IFE, DPs induce epidermal hyperplasia and rearrangements with complex DP-IFE structures forming as early as day 7 (n=5 per time point). Representative images are shown. **(e-g)** DPs and IFE often undergo extensive remodeling, with IFE forming pocket-like invaginations and with DPs assuming elongated, tongue-like shapes by day 20 (n=5 per time point). Representative images are shown. **(h)** Three-dimensional serial section reconstruction demonstrates the extent of DP-IFE remodeling on day 20. **(i, j)** In some instances, DPs remained in the granulation tissue and formed long pegs extending toward IFE. **(k)** DPs and IFE seldom formed complex structures, morphologically reminiscent of the hair peg stage of normal HF morphogenesis. Size bars: b-g, i-k – 20 μm.

Author Manuscript Author Manuscript Author Manuscript Author Manuscript

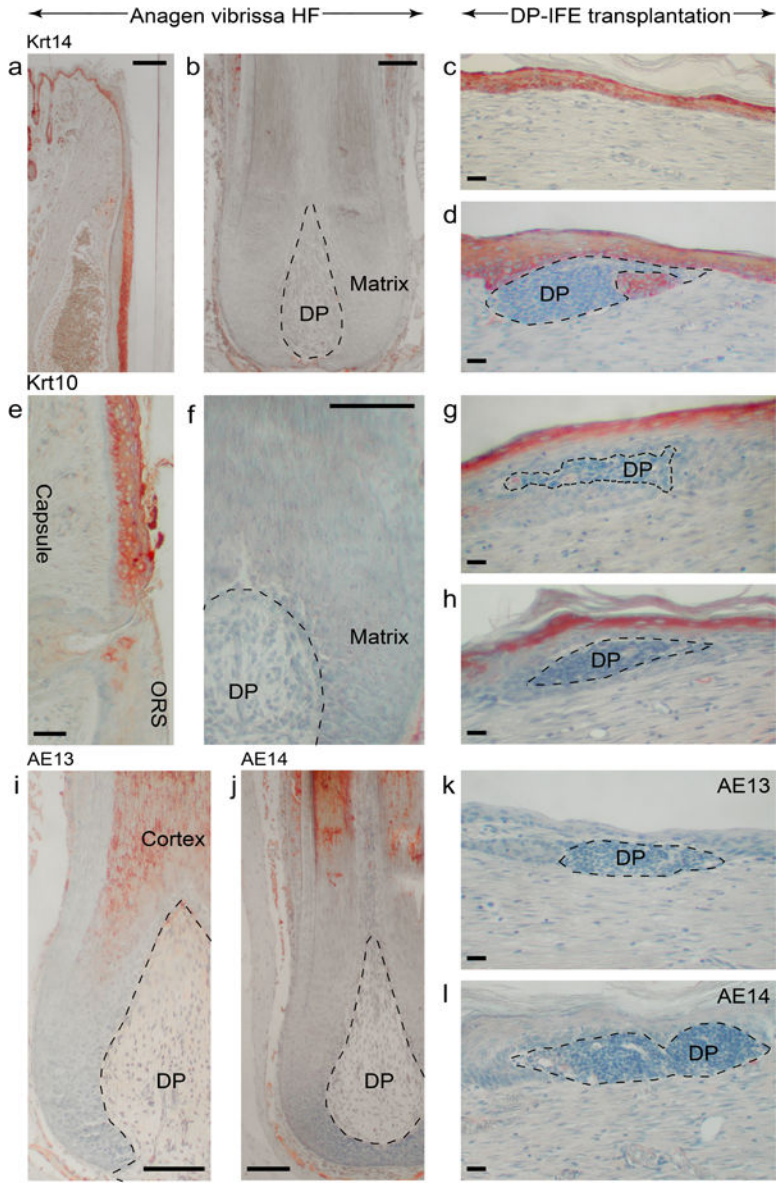

Figure 4: Dermal papillae fail to alter keratin expression patterns of transplanted epidermis.
(a, b) In normal vibrissa HFs, Krt14 is expressed in the basal layer of infundibulum, suprabasal ORS layers and is absent from hair matrix and precortex. **(c, d)** In the wound, IFE at the sites of interaction with DP maintains strong Krt14 expression. Representative images are shown. **(e, f)** In normal vibrissa HFs, Krt10 is restricted to the suprabasal layers of infundibulum and distinctly lacks from hair matrix and precortex. **(g, h)** Unlike hair matrix, Krt10 expression remains strong in the DP-IFE structures. Representative images are shown. **(i-l)** Hair cortex cytokeratin markers AE13 **(i)** and AE14 **(j)** are distinctly absent from the DP-IFE structures **(k, l)**. Representative images are shown. Size bars: a-b, f, i-j – 100 μm; c-e, g-h, k-l – 20 μm.

Author Manuscript Author Manuscript Author Manuscript Author Manuscript

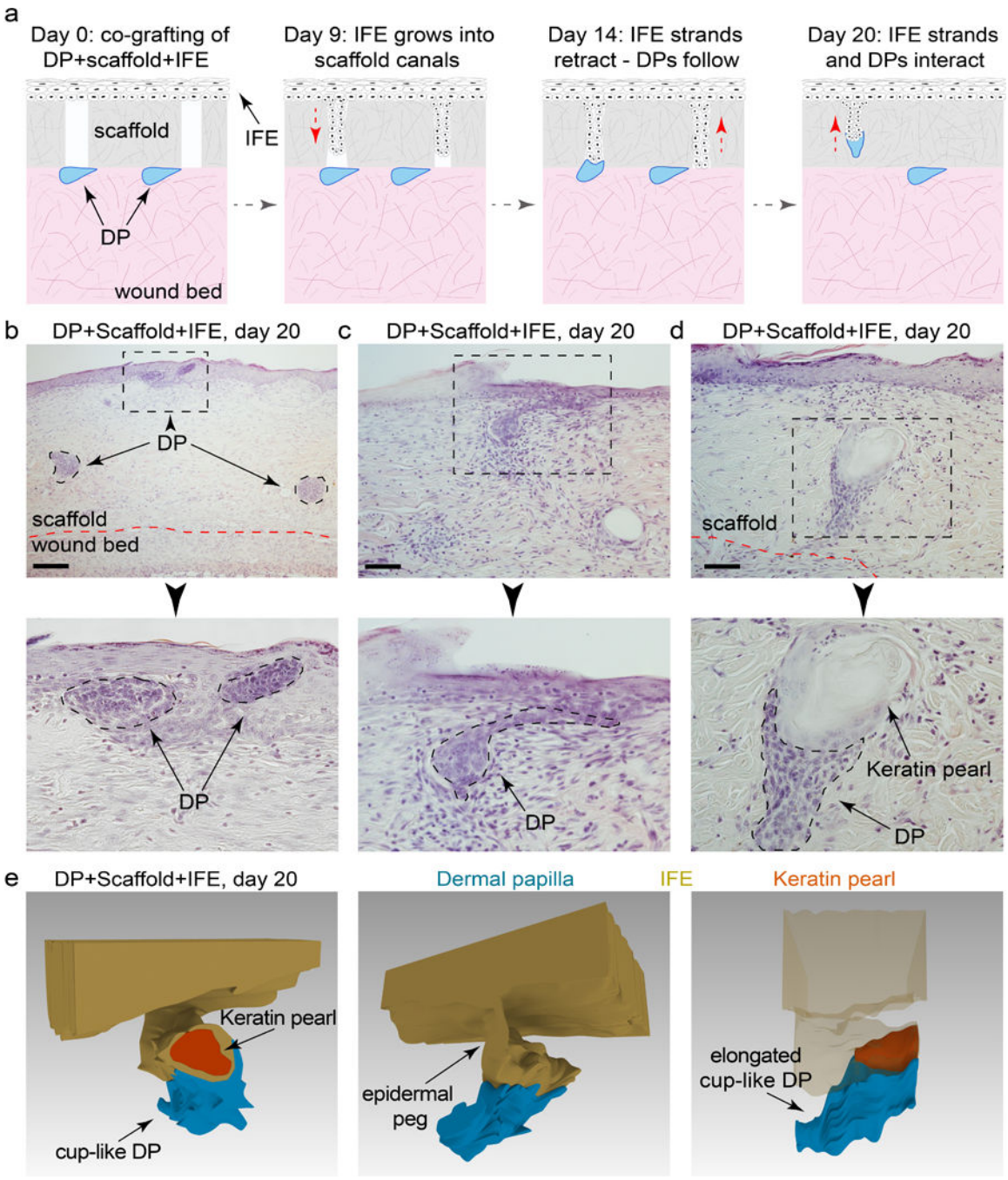

Figure 5: The complexity of dermal papilla-epidermal interactions increases in the presence of acellular scaffolds.

(a) In the modification of the wound model that includes an acellular dermal scaffold, grafted IFE invaded vacant canals of the scaffold from above, while DPs entered into the scaffold's canals from below. **(b-e)** In some instances, DP and IFE interacted within the canals producing complex three-dimensional structures. However, these structures maintained an epidermal differentiation program, evident by the formation of keratin pearls. Representative images are shown. Size bars: b –100 μm; c, d – 50 μm.

Author Manuscript Author Manuscript Author Manuscript Author Manuscript

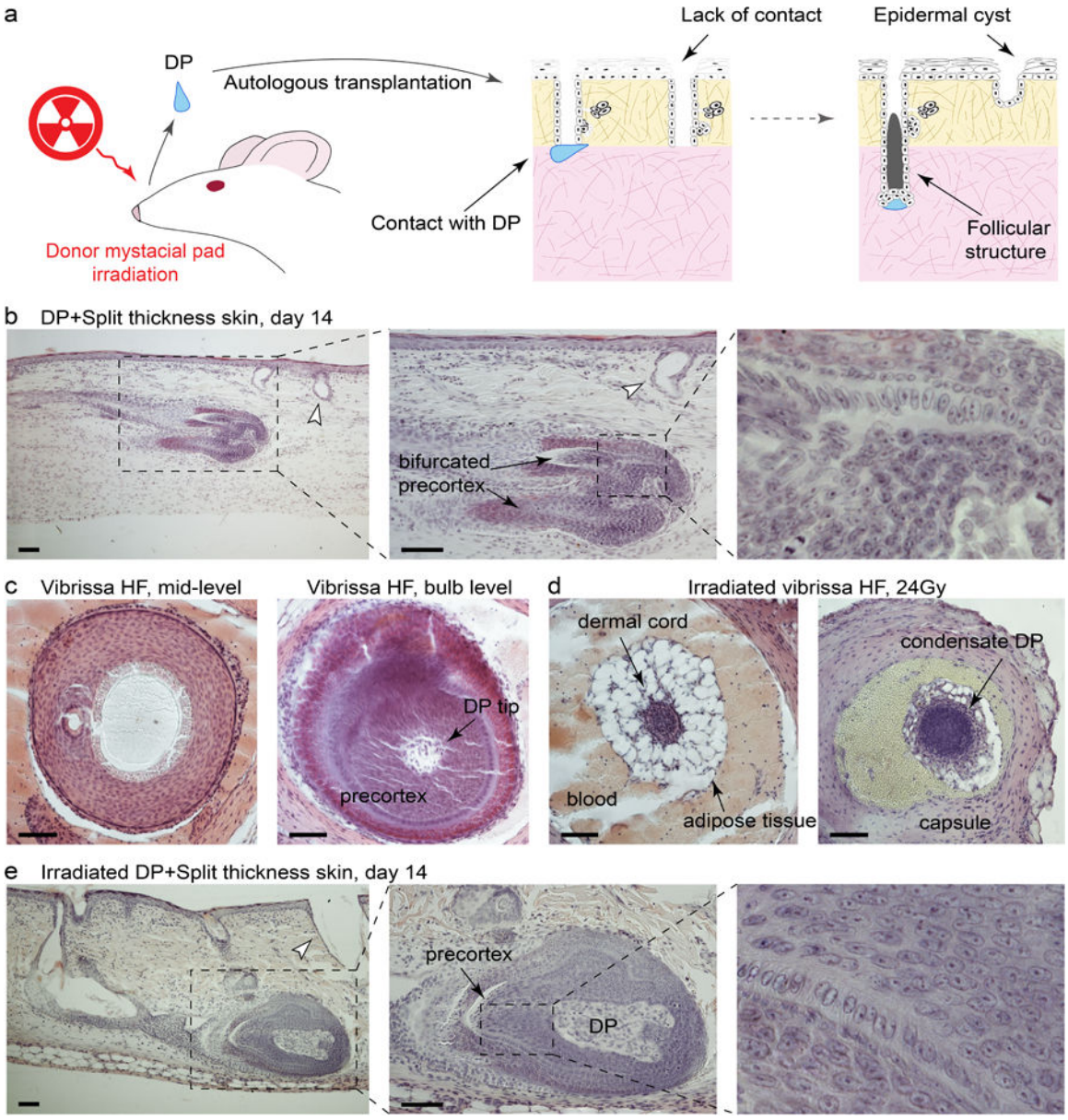

Figure 6: Dermal papillae induce hair follicle neogenesis from adult hair fated epithelium.

(a) Model of autologous transplantation using DPs and split-thickness skin graft. **(b)** DPs consistently induced giant, often bifurcated, vibrissa-like HFs from the distal segments of anagen pelage HFs. Representative images are shown. **(c-e)** In this wound model, HF neogenesis was induced by DPs derived from vibrissa HFs previously irradiated with 24 Gy of X-ray. Although this X-ray dose causes destruction of HF epithelium, DPs survive the irradiation **(c** *vs.* **d)**. Pelage HF segments not in contact with vibrissa DPs fail to regenerate new HFs (arrowheads on **b, e**). Representative images are shown. Size bars: b-e – 50 μm.